THE JOURNAL OF BIOLOGICAL CHEMISTRY VOL. 286, NO. 18, pp. 15875–15882, May 6, 2011

Moderate Calcium Channel Dysfunction in Adult Mice with Inducible Cardiomyocyte-specific Excision of the *cacnb2* Gene*

Received for publication, February 3, 2011 Published, JBC Papers in Press, February 28, 2011, DOI 10.1074/jbc.M111.227819

Marcel Meissner[‡1], Petra Weissgerber[‡1], Juan E. Camacho Londoño[‡1], Jean Prenen[§1], Sabine Link[‡], Sandra Ruppenthal[¶], Jeffery D. Molkentin[‖], Peter Lipp[¶], Bernd Nilius[§], Marc Freichel[‡], and Veit Flockerzi[‡2]

From the [‡]Experimentelle und Klinische Pharmakologie und Toxikologie, Universität des Saarlandes, 66421 Homburg, Germany, the [§]Departement Moleculaire Celbiologie, Laboratorium voor Ionenkanaalonderzoek, Katholieke Universiteit Leuven, 3000 Leuven, Belgium, the [¶]Molekulare Zellbiologie Universität des Saarlandes, 66421 Homburg, Germany, and the [‖]Department of Pediatrics, Cincinnati Children's Hospital Medical Center, University of Cincinnati, Cincinnati, Ohio 45229-3039

The major L-type voltage-gated calcium channels in heart consist of an α1C ($Ca_V1.2$) subunit usually associated with an auxiliary β subunit ($Ca_V\beta2$). In embryonic cardiomyocytes, both the complete and the cardiac myocyte-specific null mutant of $Ca_V\beta2$ resulted in reduction of L-type calcium currents by up to 75%, compromising heart function and causing defective remodeling of intra- and extra-embryonic blood vessels followed by embryonic death. Here we conditionally excised the $Ca_V\beta2$ gene (*cacnb2*) specifically in cardiac myocytes of adult mice (KO). Upon gene deletion, $Ca_V\beta2$ protein expression declined by >96% in isolated cardiac myocytes and by >74% in protein fractions from heart. These latter protein fractions include $Ca_V\beta2$ proteins expressed in cardiac fibroblasts. Surprisingly, mice did not show any obvious impairment, although *cacnb2* excision was not compensated by expression of other $Ca_V\beta$ proteins or changes of $Ca_V1.2$ protein levels. Calcium currents were still dihydropyridine-sensitive, but current density at 0 mV was reduced by <29%. The voltage for half-maximal activation was slightly shifted to more depolarized potentials in KO cardiomyocytes when compared with control cells, but the difference was not significant. In summary, $Ca_V\beta2$ appears to be a much stronger modulator of L-type calcium currents in embryonic than in adult cardiomyocytes. Although essential for embryonic survival, $Ca_V\beta2$ down-regulation in cardiomyocytes is well tolerated by the adult mice.

The L-type calcium channels in heart are high voltage-activated, and their minimal composition includes the pore-forming $Ca_V1.2\alpha_1$ subunit and the auxiliary $Ca_V\beta2$ subunit (1). $Ca_V\beta$ subunits are believed to enhance the trafficking of the channels to the plasma membrane and to produce shifts in the voltage dependence of channel activation. From the four mammalian genes coding for $Ca_V\beta$ subunits, the *cacnb2* gene is predominantly expressed in the heart (2). Overexpressing the rat neuronal $Ca_V\beta2a$ transgene in cardiomyocytes showed increased Ca^{2+} entry and progressive cell necrosis that led to pump dysfunction and premature death (3). Generation of a ubiquitous and a cardiomyocyte-specific null mutant of *cacnb2* (4) causes early embryonic death because of a morphologically and functionally compromised heart. In contrast, targeted deletion of the *cacnb1* or *cacnb3* genes and the functional inactivation of *cacnb4* caused by the spontaneous lethargic (*lh*) mutation appear not to effect cardiac function (5). In $Ca_V\beta2$ null cardiomyocytes at the embryonic days preceding death, the calcium current was reduced to approximately one-fourth to one-third of the current in wild type cells (4). The remaining calcium current was ineffective to support cardiomyocyte contraction and cardiac pump function; as a consequence, embryonic heart failure associated with pericardial effusion and, finally, embryonic death after embryonic day 10.5 occurred (4). Although it was still sensitive to dihydropyridines (4), the remaining current appears not to depend on the presence of the $Ca_V\beta2$ subunit.

To study the impact of $Ca_V\beta2$ deletion in the heart of adult animals, we induced excision of the *cacnb2* gene in cardiomyocytes of adult mice. We show that $Ca_V\beta2$ protein expression declined by >96% in isolated cardiomyocytes following gene deletion and, surprisingly, we observed only moderately impaired L-type calcium currents with a <29% reduction in current density. Different from the embryo, $Ca_V\beta2$ protein expression is not essential for L-type calcium currents in adult cardiomyocytes and survival of the adult mouse.

EXPERIMENTAL PROCEDURES

Animal Care and Generation of Inducible and Cardiomyocyte-specific $Ca_v\beta2$ deletion in Mice—The $Ca_V\beta2^{flox/flox}$ mouse (4) (mixed background of C57BL/6 × 129/SvJ) was crossed with the $Ca_V\beta2^{+/-}$ mouse (4) to obtain the $Ca_V\beta2^{flox/-}$ mouse. The latter was crossed with an α-MHC-MerCreMer mouse (6) expressing a Tamoxifen-inducible Cre recombinase protein fused to two mutant estrogen receptor ligand-binding domains (MerCreMer) under the control of the α-myosin heavy chain

* This work was supported by Interuniversity Attraction Poles Programme – Belgian State – Belgian Science Policy, P6/28, the Research Council of the KU Leuven (Grant GOA 2004/07), the Flemish Government (Excellentiefinanciering, Grant EF/95/010) (to B. N. and J. P.), the Deutsche Forschungsgemeinschaft (Grants SFB530, KFO196, and GK 1326 (to P. L., M. F., and V. F.), Grant SFB894 (to P. W., M. F., and V. F.), the Homburger Forschungsförderungsprogramm HOMFOR (P. L., M. M., P. W., M. F., and V. F.), and the Forschungskommission der Universitaet des Saarlandes (P. L., M. F., and V. F.).

[1] These authors contributed equally to this work.

[2] To whom correspondence should be addressed: Experimentelle und Klinische Pharmakologie und Toxikologie, Gebäude 46, 66421 Homburg, Germany. Fax: 49-6841-1626402; E-mail: veit.flockerzi@uks.eu.

promoter to obtain the $Ca_V\beta 2^{flox/-}$/MerCreMer$^{tg/0}$ mouse, which allows for inducible, cardiomyocyte-specific disruption of the *Cacnb2* gene in adult mice. *Cacnb2* gene excision in 10–12-week-old mice to obtain $Ca_V\beta 2^{flox/-}$/MerCreMer$^{tg/0}$ knock-out (KO) mice was accomplished by i.p. administration of Tamoxifen (60 mg/kg) for 5 consecutive days in week 1 and week 3. Tamoxifen was freshly dissolved in Mygliol 812 oil (Caelo) at a concentration of 20 mg/ml. Wild type mice, $Ca_V\beta 2^{flox/-}$ mice, and $Ca_V\beta 2^{flox/-}$/MerCreMer$^{tg/0}$ mice injected with Mygliol 812 oil only (mock) served as controls. Hearts were harvested at weeks 6, 9, and 12 following Tamoxifen administration. All animal procedures were performed in accordance with German legislation on the protection of animals and approved by the Saarland's Institutional Animal Care and Use Committee.

Organs of Tamoxifen-injected mice were obtained under terminal Avertin (2,2,2-tribromoethanol, Fluka) anesthesia. Briefly, the abdominal and thoracic cavities were exposed, and the renal artery was punctured to reduce the blood flow going to the heart. The heart was quickly excised and placed into ice-cold saline solution, where the excess of fat tissue and surrounding vessels was removed. Immediately, the lungs and liver were dissected from the mouse and placed into a Petri dish. Before weighing the organs, the excess of blood was gently removed by placing the organs into a paper tissue. Each organ was weighed (wet weight), the hearts were saved for Western blots, and the lungs and liver were dried at 70 °C over 48 h to get the dry weight. The tibia was removed, carefully cleaned from skin and muscle, and measured out.

Antibodies and Western Blots—Microsomal membrane protein fractions from heart and brain were solubilized with Laemmli buffer, denatured, and subjected to SDS-PAGE. Proteins were transferred onto a nitrocellulose membrane (Hybond-C Extra, GE Healthcare) and probed with antibodies for $Ca_V\beta$ (in-house generated antibodies 424 and 425 (anti-mouse $Ca_V\beta 2$ (4)), 237 (anti-mouse $Ca_V\beta 1$ (7)), 828 and MM2 (anti-mouse $Ca_V\beta 3$ (8)), and 830 and 1051 (anti-mouse $Ca_V\beta 4$ (9)), $Ca_V1.2$ (kindly provided by Dr. Franz Hofmann, München, Germany), GAPDH (Santa Cruz Biotechnology), P4HB (Acris 11245-1-AP), α-actinin (Sigma A 7811), and ryanodine receptor (Thermo Scientific). Specificity of $Ca_V\beta$ antibodies was confirmed by using microsomal membrane protein fractions from wild type mice and mice deficient in $Ca_V\beta 2$, $Ca_V\beta 3$, and $Ca_V\beta 4$ (the *lh* mouse, respectively). Proteins were detected using horseradish peroxidase-coupled secondary antibodies and the Western Lightning chemiluminescence reagent *Plus* (PerkinElmer Life Sciences). Original scans were saved as TIFF files from LAS 3000 (Fujifilm), which were further processed in Adobe Photoshop. Images were cropped, resized proportionally, and brought to the resolution required for publication.

Isolation of Mouse Cardiac Cells and Primary Culture of Cardiac Fibroblasts—Ventricular cells were obtained from dissociated hearts of female adult wild type mice (F1 between C57Bl/6N × 129/SvJ, 10 weeks). Mice were anesthetized by intraperitoneal injection of Avertin (0.5 mg/g of body weight) including heparin (20 units/g of body weight) to avoid blood clots; the hearts were quickly removed via thoracotomy and transferred to an ice-cold modified Tyrode's solution (TS),[3] containing (in mM): 134 NaCl; 4 KCl; 1.2 $MgSO_4$; 1.2 Na_2HPO_4; 10 HEPES; 11 glucose; pH 7.36. After that, the hearts were cannulated via the aorta, attached to a Langendorff apparatus, and perfused retrogradely with carbogen (5% CO_2, 95% O_2)-saturated TS containing 200 μM EGTA and 10 mM 2,3-butanedione-monoxime for 7 min. The perfusion solution was then changed to constantly gassed (carbogen) TS containing a collagenase/protease mixture (Liberase TM, Roche Applied Science) at a final concentration of 133 μg/ml for 5–6 min. The ventricles were isolated, dissected, and transferred to TS supplemented with 4% bovine serum albumin (BSA), 12.5 μM Ca_2Cl, and 1.4 ng/ml DNase I (Sigma). The ventricles were cut into small pieces followed by homogenization of the tissue by gently pipetting. The suspension was filtered through a nylon filter (pore size 150 μm) and maintained for 10 min in the same solution for sedimentation; cardiomyocytes were mainly concentrated in the pellet. Fibroblasts remaining in the supernatant were collected by centrifugation (250 × *g*, 10 min) and washed once in M199 medium (Invitrogen). They were seeded on a 25-cm^2 culture flask (one heart per flask), and the medium was changed every 24 h until the cells were confluent; the cells were split by trypsin (Invitrogen) treatment and harvested between passages 1 and 2 for RNA isolation or Western blot analysis. The cardiomyocytes contained in the pellet were resuspended in TS solution containing BSA, Ca_2Cl, and DNase and were transferred into a polystyrene culture dish; then, they were incubated (37 °C in 5% CO_2) for 2 h to remove adherent cells, and the non-attaching cardiomyocytes were saved. The cardiomyocytes were collected by centrifugation (40 × *g*, 1.5 min) and subsequently resuspended in ice-cold Ca^{2+}/Mg^{2+}-free Dulbecco's PBS (Invitrogen) and washed twice, the first time by centrifuging at 40 × *g* (1.5 min) and the second time at 40 × *g* (1 min) to remove debris and possible remaining blood cells. The final pellet was snap-frozen in liquid nitrogen and maintained at −80 °C until protein isolation for Western blots.

Cardiomyocytes for laser capture microdissection (LCM) were obtained as described before. The cardiomyocytes were washed and resuspended in sterile ice-cold Ca^{2+}/Mg^{2+} free Dulbecco's PBS, and then they were cytospun on LCM glass slides covered by 1-mm PEN membrane (Zeiss) and directly fixed by immersion in absolute methanol for 1 min. The samples were kept on ice inside 50-ml polypropylene tubes to avoid complete drying until cardiomyocyte isolation. The collection of the cells was performed using a Zeiss P.A.L.M. LCM microscope (Zeiss/Microlaser Technologies) with a 20× objective (Plan-NEOFLUAR 0.5 ∞/0.17). Cardiomyocytes were collected in 0.5-ml LCM tubes (AdhesiveCap 500 opaque, Zeiss). Cardiomyocytes were identified by their morphology; only isolated and well preserved and rod-shaped cells were chosen for LCM. About 60 cardiomyocytes were collected per cap; cells were lysed in Buffer RLT (Qiagen), frozen in dry ice, and kept at −80 °C until RNA extraction. For RT-PCR, RNA from four caps (227 cells) was pooled.

[3] The abbreviations used are: TS, Tyrode's solution; LCM, laser capture microdissection; pF, picofarads; nS, nanosiemens; het, heterozygous; RyR, ryanodine receptor.

RT-PCR—Total RNA was extracted using the RNeasy micro kit (Qiagen). We used 40 ng of total RNA from cardiomyocytes and complete heart and 80 ng of total RNA from cardiac fibroblasts for one-step RT-PCR (Invitrogen). The following intron-spanning primers were used for amplification of $Ca_V\beta 2$ fragments: mb2_32 (5′-GTT CGG CAG ACT CCT ACA CC-3′) and mb2_10 (5′-CTC TAG TTT GAC TGG GCT TGG-3′), resulting in a $Ca_V\beta 2$-specific 326-bp fragment. For amplification of the 225-bp fragment containing part of the housekeeping gene hypoxanthine-guanine phosphoribosyltransferase 1 (HPRT1) as control, we used total RNA from complete heart and the following oligonucleotides: UW_637 (5′-GCT CGA GAT GTC ATG AAGG-3′) and UW_638 (5′-AGT TGA GAG AGA TCA TCT CCA CC-3′). PCR fragments were analyzed on a 2% agarose gel.

Pulse-Chase and Immunoprecipitation Experiments—COS-7 cells were irradiated with 30 grays to prevent continuous proliferation. 24 h later, cells were transfected with $Ca_V\beta 2$ cDNA or $Ca_V\beta 2$ plus $Ca_V 1.2$ cDNAs, respectively, using FuGENE 6 (Roche Applied Science) according to the manufacturer's specifications. 24 h after transfection, cells were starved for 2 h in Met- and Cys-free DMEM-medium followed by a 2-h labeling in medium supplemented with 100 μCi of L-[^{35}S]Met and L-[^{35}S]Cys). Radioactive media were eventually washed out with PBS (time 0) and replaced with DMEM medium. Cells were harvested at time 0 and 12, 24, 48, 72, 96, and 120 h thereafter and lysed in the presence of 0.05 M Tris, 0.15 M NaCl, 0.005 M EDTA, 0.5% sodium deoxycholate, 1% Nonidet P-40, 0.1% SDS, pH 8, and $Ca_V\beta 2$ proteins were immunoprecipitated by antibody 425. The precipitated proteins were run on SDS-PAGE and transferred to nitrocellulose filters, which were analyzed by Western blotting and by exposure to PhosphorImager screens followed by quantitative analysis using the AIDA Image Analyzer software.

Immunofluorescence and Confocal Imaging—Isolated myocytes were plated onto glass coverslips precoated with extracellular matrix proteins (R&D Systems) and rinsed with PBS before fixation (4% formaldehyde in PBS, 10 min, room temperature). Thereafter cells were washed once for 10 min in PBS and permeabilized with 0.4% Triton X-100 for 10 min. After an additional 10-min washing step, they were incubated in blocking solution (PBS containing 5% bovine serum albumin) at 21 °C for 10 min. Cells were incubated with the primary antibodies for the ryanodine receptor (1:200) and $Ca_V\beta 2$ (antibody 425, 1:100) for 1 h at 21 °C. After three washes with PBS containing 0.1% Tween 20 at 21 °C, cells were incubated with secondary antibodies (DyLight 649 AffiniPure goat anti-rabbit, Jackson ImmunoResearch Europe, and ATTO 550-conjugated goat anti-mouse, Sigma) at 21 °C for 30 min. Cells were washed again under the same conditions and rinsed once with water. The coverslips were mounted on a drop of mounting medium (ProLong® Gold antifade reagent, Invitrogen) and stored at 4 °C until further analysis.

Coverslips with the labeled myocytes were transferred onto the stage of a Leica SP5-II laser scanning confocal microscope (Leica Microsystems, Wetzlar, Germany), and imaging was performed through a 63× oil immersion objective (HCX PL APO, 1.4, Leica). We used a 561 nm laser (CYA-015, Melles-Griot, Bensheim, Germany) and a 633 nm laser (He-Ne, Lasos, Jena, Germany) to excite ATTO550 and DyLight649, respectively. For detection of the fluorescence, the following two spectral bandwidths were used: 565–628 nm (for ATTO550) and 640–800 nm (for DyLight649). Settings for laser excitation as well as emission settings (spectral bandwidth, photomultiplier tube gain, offset) were kept constant between measurements. Z-stacks were acquired as series of confocal sections (each 1024 × 1024 pixels in size) interspaced by 0.15-μm steps. Resulting data were stored onto an OMERO database system (the Open Microscopy Environment) for archiving and later post processing. For analysis and composition of the figures, z-stacks were deconvolved in AutoQuant software (AutoDeblur X, MediaCybernetics), stored as 16-bit grayscale images, and imported into Adobe Illustrator CS5 for composition of final figures. Two sets of figures are provided, one optimized for screen display and another one for printing, taking into account the different results of presentation. For this, all grayscale images were treated the same, *i.e.* their look-up tables were adapted together to ensure appropriate presentation of grayscale data on a printer or the computer display and to preserve intensity differences between the images.

Electrophysiology—Mouse ventricular myocytes were isolated by using a Langendorff perfusion technique as described previously (10) but adapted for mice. In short, Langendorff hearts were perfused 6 min with a Ca^{2+}-free solution and afterward for 15 min with an enzyme solution (Ca^{2+}-free and 1 mg/ml collagenase A (Roche Applied Science) supplemented with 0.1 mg/ml protease XIV (Sigma)). After cutting the heart into small pieces of ~2 mm^3, these remainders were washed with a Krebs solution (see below) but with 0.18 mM $CaCl_2$ to obtain isolated single cells, which were used for the experiments.

Whole cell voltage clamp recordings were obtained using a ruptured patch clamp with an EPC9 patch clamp amplifier (HEKA Electronics, Lambrecht/Pfalz, Germany). For control of voltage-clamp protocols and data acquisition, we used the pCLAMP 9 software (Molecular Devices, Foster City, CA) run on an IBM-compatible PC, which was connected to the amplifier via a TL-1 DMA interface (Molecular Devices). Patch pipettes (1–2.5 megaohms) were pulled from Vitrex capillary tubes (Modulohm) using a DMZ universal puller (Zeitz Instruments). Series resistance was compensated to the maximum extent possible (40–60%). An Ag-AgCl wire was used as reference electrode. Membrane capacitive transients were electronically compensated, and the linear background components were digitally subtracted when possible before data analysis. In the case of tail current measurements, linear background components and capacitive transients were subtracted. Current traces were filtered at 1 kHz and digitized at 5 kHz. Potentiation of L-type Ca^{2+} currents was achieved by the application of 1 μM BayK-8644, and inhibition was achieved by 2 μM nifedipine (both from Bayer Leverkusen). All experiments were performed at 22–25 °C.

In all experiments, a bath (Krebs) solution was used (in mM): 156 CsCl; 1.5 $CaCl_2$; 1 $MgCl_2$; 10 HEPES; 10 glucose; adjusted with CsOH to pH 7.4. This solution also nulled the membrane

potential of the myocytes. The following pipette solution was used (in mM): 130 CsCl; 20 tetraethylammonium chloride; 1 $MgCl_2$; 1 EGTA; 5 Na_2ATP; 0.1 GTP; 5 Hepes adjusted with CsOH to pH 7.2.

Voltage step protocols were applied from a holding potential of −80 mV for 200 ms to a prepulse of −40 mV followed by a 300-ms test pulse between −50 and +80 mV. For inactivation, from a holding potential of −80 mV, prepulses of 300 ms were applied from −90 to 0 mV with an increment of +10 mV. Currents after the prepulse were measured at 0 mV. In all protocols, the interval between the pulse protocols was 2 s.

The data were analyzed using WinASCD (24). IV curves and inactivation curves were fitted by

$$I = \frac{G_{max} \times (V - V_{rev})}{1 + \exp(-(V - V_{1/2,act})/s_{act})} \quad \text{(Eq. 1)}$$

where I (pA/pF) is the measured current at the test potential V (in mV), and the fitted parameters are the maximal conductance G_{max} (nS/pF), the potential of half-maximal activation $V_{1/2,act}$ (in mV), the slope of activation s_{act} (in mV), and the reversal potential V_{rev} (in mV). Inactivation was fitted by

$$I = \frac{I_{max}}{1 + \exp((V - V_{1/2,inact})/s_{inact})} \quad \text{(Eq. 2)}$$

where I is the measured current after the prepotential at 0 mV, I_{max} is the maximal current at 0 mV and at the prepotential of −90 mV, V is the prepotential, $V_{1/2,inact}$ is the potential for 50% inactivation, and s_{inact} is the slope factor for inactivation. For the statistical analysis, the two-side *t* test was applied (<0.05 considered significant), and one-way analysis of variance was followed by multiple comparisons-Holm-Sidak *t* test.

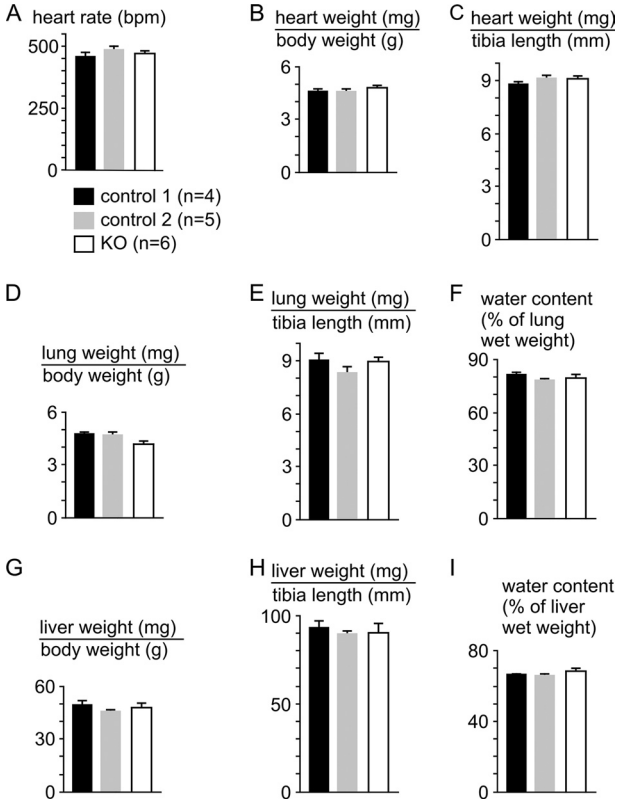

FIGURE 1. **KO mice ($Ca_V\beta2^{-/flox}$/MerCreMer$^{tg/0}$ mice after induction for *cacnb2* gene deletion by Tamoxifen), like controls receiving identical Tamoxifen treatment, did not exhibit any signs of cardiac decompensation.** *A–I*, heart rate (*A*), heart weight (*B* and *C*), lung weight (*D* and *E*), liver weight (*G* and *H*), and lung (*F*) and liver water content (*I*) (given as the percentage of organ wet weight) were not significantly different among the three genotypes. *Control 1*, $Ca_V\beta2^{+/flox}$/MerCreMer$^{tg/0}$; *control 2*, $Ca_V\beta2^{-/flox}$. Values are shown as mean ± S.E.

RESULTS AND DISCUSSION

Different from the $Ca_V\beta2^{-/-}$ mice and mice with a cardiomyocyte-restricted excision of the *Cacnb2* gene, which died *in utero* (4), $Ca_V\beta2^{+/-}$ (4), $Ca_V\beta2^{flox/flox}$ (4), $Ca_V\beta2^{-/flox}$, and $Ca_V\beta2^{-/flox}$/MerCreMer$^{tg/0}$ mice were born healthy and did not exhibit any obvious abnormalities during adulthood. KO mice ($Ca_V\beta2^{-/flox}$/MerCreMer$^{tg/0}$ at 6, 9, or 12 weeks after induction for *cacnb2* gene deletion by Tamoxifen) also appeared healthy and did not exhibit any obvious abnormalities or symptoms of cardiac decompensation (Fig. 1). The heart rate (Fig. 1*A*) and heart weight (Fig. 1, *B* and *C*), the lung and liver weights (Fig. 1, *D*, *E*, *G*, and *H*), as well as the water content of lung and liver (Fig. 1, *F* and *I*) were not different between KO mice or the controls (control 1, $Ca_V\beta2^{+/flox}$/MerCreMer$^{tg/0}$; control 2, $Ca_V\beta2^{-/flox}$).

In brain, all four $Ca_V\beta$ subunits are expressed (Fig. 2*A*), whereas in adult heart, only the $Ca_V\beta2$ protein is detectable (Fig. 2*B*). $Ca_V\beta2$ expression levels in heart were not different among the various genotypes (Fig. 2, *C* and *D*) but was different in heart from KO mice, where $Ca_V\beta2$ transcript expression was hardly detectable (Fig. 2*C*) and protein expression was significantly reduced (Fig. 2*D, lane 4*), indicating that the MerCreMer transgene is tightly regulated within the heart in the absence of Tamoxifen and that $Ca_V\beta2$ expression in the heart can be effectively controlled by Tamoxifen-induced *cacnb2* gene excision, as expected (6, 11). $Ca_V\beta1$, $Ca_V\beta3$, and $Ca_V\beta4$ proteins were not detectable, and the expression level of $Ca_V1.2$ was not changed (Fig. 2*D*). All Ca_V proteins were still being detectable in brain (Fig. 2*D*, *lanes 5* and *6*), indicating that there was no apparent compensatory expression of these Ca_V subunits in the heart of KO mice.

Tamoxifen treatment resulted in a significant reduction of the $Ca_V\beta2$ protein immunoreactivity in heart, and to estimate the amount of remaining protein, we performed experiments like the one shown in Fig. 2*E*, employing two independent antibodies for $Ca_V\beta2$. The amount of $Ca_V\beta2$ protein remaining in hearts from KO mice ($n = 46$) was 21.8 ± 5.7% (antibody 425) and 25.9 ± 7.5% (antibody 424) when compared with controls ($n = 46$). These values are in agreement with the Tamoxifen-induced Cre-mediated recombination frequency of >70% in heart revealed by Southern blot analysis (6). Part of the remaining $Ca_V\beta2$ proteins may therefore be expressed in non-myocytes, which are present in heart at a fair number (6, 16).

$Ca_V\beta2$ immunoreactivity (Fig. 3*A*, *right column*) in isolated cardiomyocytes from control mice shares the typical cross-striation pattern with the ryanodine receptor type 2 (RyR2) immunoreactivity (Fig. 3, *A* and *B*, *left columns*), reflecting the spatial juxtaposition of the voltage-gated calcium channels and the ryanodine receptors. In myocytes from KO mice, the $Ca_V\beta2$ immunoreactivity is considerably reduced (Fig. 3*B*, *right col-*

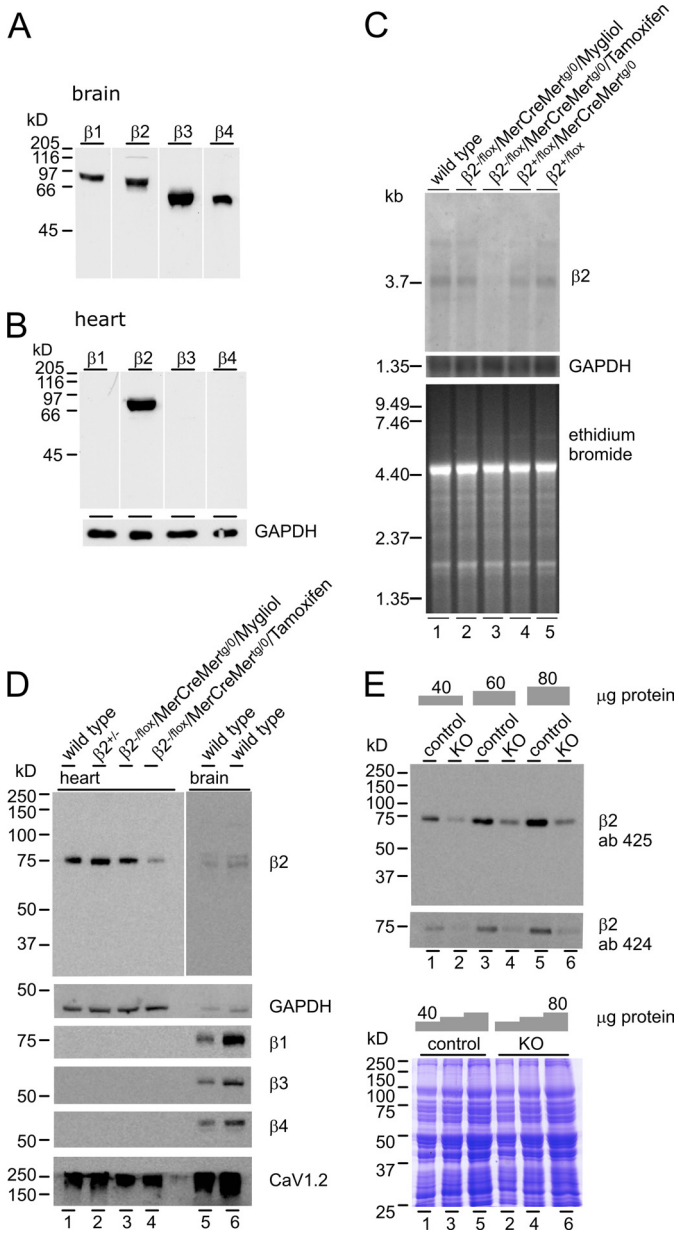

FIGURE 2. **$Ca_v\beta$-expression.** *A* and *B*, $Ca_V\beta 1$($\beta 1$), $Ca_V\beta 2$($\beta 2$), $Ca_V\beta 3$($\beta 3$), and $Ca_V\beta 4$($\beta 4$) in brain (*A*) and expression of $Ca_V\beta 2$ in heart (*B*) (100 μg/lane). *C*, $Ca_V\beta 2$ transcript expression in cardiac poly(A^+)-RNA (10 μg/lane) from WT (*lane 1*), $Ca_V\beta 2^{-/flox}$/$MerCreMer^{tg/0}$ (mock, *lane 2*), Tamoxifen-treated $Ca_V\beta 2^{-/flox}$/$MerCreMer^{tg/0}$ (KO, *lane 3*), $Ca_V\beta 2^{+/flox}$/$MerCreMer^{tg/0}$ (*lane 4*), and $Ca_V\beta 2^{+/flox}$/$MerCreMer^{0/0}$ (*lane 5*). Loading controls are as follows: GAPDH expression (*middle*) and ethidium bromide stain (*bottom*). *D*, $Ca_V\beta 2$ protein expression in heart (45 μg) from WT (*lane 1*), $Ca_V\beta 2^{+/-}$ (*lane 2*), $Ca_V\beta 2^{-/flox}$/$MerCreMer^{tg/0}$ (mock, *lane 3*), and Tamoxifen-treated $Ca_V\beta 2^{-/flox}$/$MerCreMer^{tg/0}$ (KO) (*lane 4*). *Lane 5*, 40 μg; lane *6*, 80 μg. Protein expression in brain is shown as control (exposed for 15 min when compared with 1 min (*lanes 1–4*)). GAPDH was used as a loading control. *E*, estimation of the $Ca_V\beta 2$ protein expression levels in hearts from controls (*lanes 1*, *3*, and *5*) and KO (*lanes 2*, *4*, and *6*) using the $Ca_V\beta 2$ antibodies 425 (*upper*) and 424 (*lower*). Coomassie Brilliant Blue stain was used as a loading control.

umn), whereas the RyR2 immunoreactivity is unchanged (Fig. 3*B*, *left column*). To estimate the amount of the remaining $Ca_V\beta 2$ protein in isolated KO cardiomyocytes, we performed Western blots using lysates from these cells (Fig. 3, *C* and *D*). The amount of $Ca_V\beta 2$ protein left in isolated myocytes from KO mice was 3.7 ± 0.9% (three independent blots) of the amount present in control cells (Fig. 3, *C* and *D*) and much less than the 21.8–25.9% detectable in protein fractions from KO hearts (Fig. 2*E*). Apparently, $Ca_V\beta 2$ protein is also expressed in non-myocyte cellular components of the heart. By using RT-PCR, we could identify $Ca_V\beta 2$ transcripts (Fig. 3*E*, *lane 4*) and proteins in three independent preparations of early passage cardiac fibroblasts (Fig. 3*F*, *lanes 3–5*).

The hallmarks of $Ca_V\beta$ function are an increase in current density and a shift in voltage dependence of activation toward more hyperpolarized potentials (1). In isolated adult cardiomyocytes, L-type calcium currents are readily detectable (Fig. 4). Whole cell current density ($I_{Ca,0mV}$) and maximal whole cell conductance (G_{max}) were reduced from −9.1 ± 0.64 pA/pF (control, $n = 9$) to 6.5 ± 0.44 pA/pF (KO, $n = 8$), *i.e.* by 28.6% ($I_{Ca,0mV}$) (Fig. 4*E*) and from 0.19 ± 0.02 nS/pF (control, $n = 9$) to 0.15 ± 0.02 nS/pF (KO, $n = 8$), *i.e.* by 21.1% (G_{max}). Although the potential of half-maximal activation was slightly shifted to more depolarized potentials in KO cardiomyocytes ($V_{½,act}$, −10.8 ± 0.9 mV; $n = 7$) when compared with control cells ($V_{½,act}$, −12.1 ± 1.1 mV, $n = 9$), the difference was not significant (Fig. 4*E*). Similarly, the kinetics of inactivation is not significantly different between control and KO for all potentials (Fig. 4, *F*, *G*, and *H*). Currents of either group were sensitive to dihydropyridines (Fig. 5) with Bay-K8644 increasing current densities of $I_{Ca,0mV}$ in KO cells to −8.0 ± 0.55 pA/pF ($n = 7$) (Fig. 4*D*), *i.e.* by 23.1% when compared with the current density in the absence of Bay-K8644, and to −11.3 ± 0.72 pA/pF, *i.e.* by 24.2% in control cells (Fig. 5*C*, $n = 7$), and with nifedipine inhibiting $I_{Ca,0mV}$ to −3.5 ± 0.47 pA/pF, *i.e.* by 46.2% (KO cells, $n = 7$) and to −3.4 ± 0.31 pA/pF, *i.e.* by 62.6% (control cells). The channel agonist Bay-K8644 induced in cells of both genotypes a significant shift in the potential of half-maximal activation ($V_{½,act}$) toward more negative potentials, from −12.1 ± 1.1 to −16.2 ± 1.4 mV (controls) and from −10.8 ± 0.9 to −15.3 ± 1.2 mV (KO); no differences in shift were obtained by comparing both groups.

In another set of experiments, we compared wild type (WT) and $Ca_V\beta 2^{+/-}$ mice (het). The $I_{Ca,0mV}$ and the G_{max} were not significantly different ($I_{Ca,0mV}$, WT, −8.2 ± 0.7 pA/pF, $n = 27$; het, −8.8 ± 0.9 pA/pF, $n = 7$; G_{max}, WT, 0.19 ± 0.11 nS/pF, $n = 26$; het, 0.21 ± 0.16 nS/pF, $n = 7$). Parameters of activation ($V_{½,act}$, WT, −10.8 ± 0.6 mV, $n = 27$; het, −10.4 ± 1.4 mV, $n = 7$; s, WT, 6.4 ± 0.31 mV; het, 5.8 ± 0.40 mV) and inactivation ($V_{½,inact}$, WT, −29.2 ± 0.7 mV, $n = 26$; het, −27.4 ± 1.2 mV, $n = 7$; s, WT, 6.9 ± 0.34 mV; het, 7.4 ± 0.45 mV) were also not statistically different.

Considering that $Ca_V\beta$ subunits may exist in pools that dynamically interact with the $Ca_V1.2$ protein (12, 13), the reduced current density could be caused by the loss of that pool responsible for trafficking and surface expression. $Ca_V\beta 2$ proteins already in complex with the plasma membrane $Ca_V1.2$ and modulating channel activation might be more stable and not require *de novo* protein synthesis. Berrow *et al.* (14) estimated a 55–60-h half-life of $Ca_V\beta$-subunits upon application of a $Ca_V\beta$ antisense oligonucleotide, and 50% of the $Ca_V1.2$ protein is degraded 25 h after the chase (15). We also performed pulse-chase experiments and could not detect a difference of the half-life of 9.5–10 h of the mouse $Ca_V\beta 2$ protein when

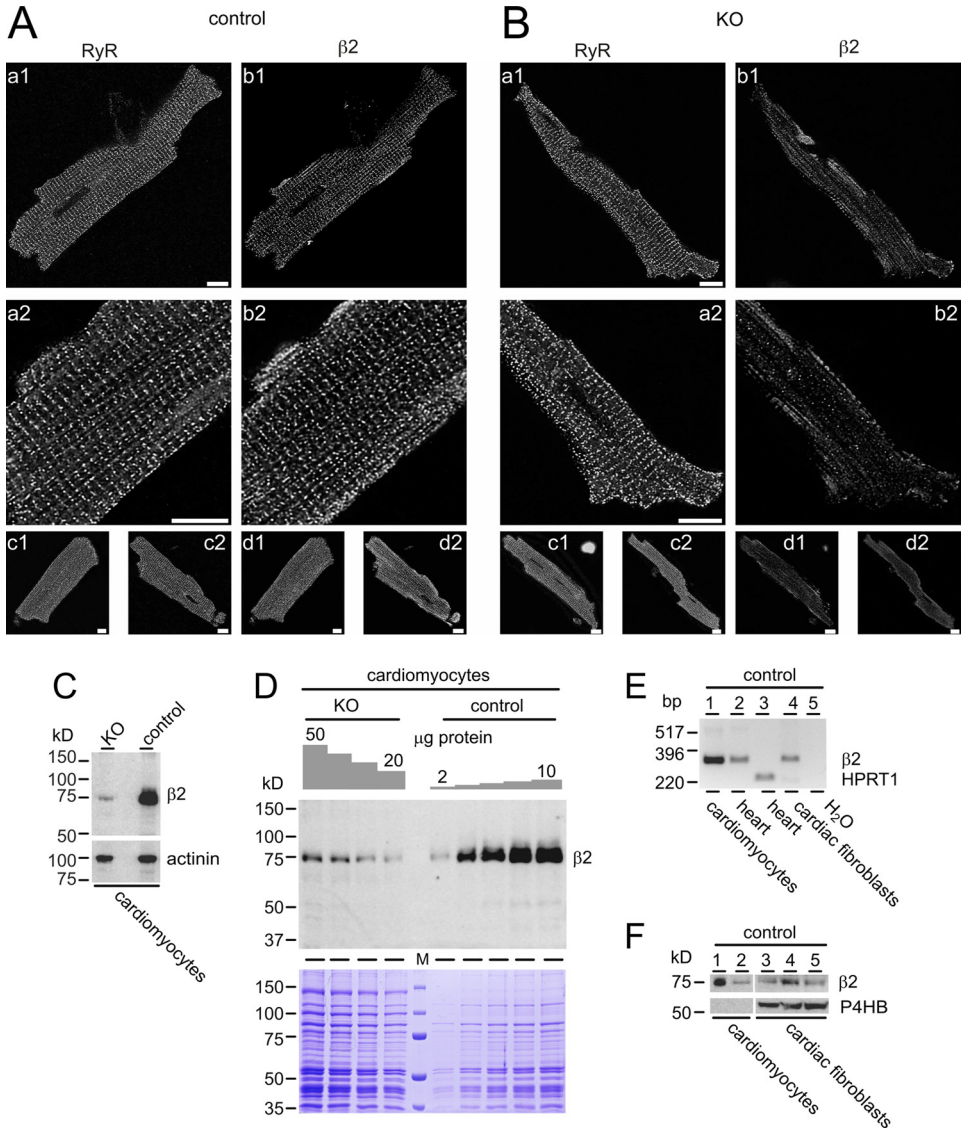

FIGURE 3. **$Ca_V\beta2$ ($\beta2$) expression in isolated cardiomyocytes and cardiac fibroblasts.** Isolated ventricular myocytes of control (*A*) and KO mice (*B*) were probed for ryanodine receptors (RyR, *left columns*) and $\beta2$ (*right columns*). During confocal imaging, the operator was blinded to the genotype of the cardiomyocytes. *A*, myocytes labeled for RyR (*panels a1* and *a2*) display the typical cross-striation pattern. Probing for $\beta2$ (*panels b1* and *b2*) in the same cell depicts a high degree of similarity in its pattern when compared with the RyR distribution. *Panels a2* and *b2* have been generated by optically zooming into the cell and rescanning the lower left part of the myocyte at a different z-position. *Panels c1*, *c2*, *d1*, and *d2*, representative overviews of RyR (*panels c1* and *c2*) and $\beta2$ (*panels d1* and *d2*) immunoreactivity of additional myocytes. *B*, the $\beta2$ immunoreactivity is almost absent in ventricular myocytes from $\beta2$-KO mice. Ventricular myocytes were treated similarly to the cells in *A*. *Scale bars* represent 10 μm. *C*, $\beta2$ protein expression in isolated cardiomyocytes (20 μg of protein/lane) from KO and from controls. Expression of α-actinin was used as a loading control. *D*, estimation of the $\beta2$ protein expression levels in isolated cardiac myocytes from controls and KO. The amount of protein applied is as indicated. Coomassie Brilliant Blue stain was used as a loading control. *M*, marker proteins. *E*, RT-PCR amplification of a specific $\beta2$ 326-bp fragment from single cardiomyocytes obtained as chippings by laser microdissection (*lane 1*, 40 ng of RNA), mouse heart (*lane 2*, 40 ng of RNA), cardiac fibroblasts (*lane 4*, 80 ng of RNA). Amplification of hypoxanthine-guanine phosphoribosyltransferase 1 (*HPRT1*, from total RNA obtained from mouse heart, *lane 3*) and PCR performed in the absence of template (H_2O, *lane 5*) served as controls. *F*, the $\beta2$ protein expression in isolated cardiomyocytes (*lane 1*, 30 μg of protein, *lane 2*, 10 μg) and in three independent cardiac fibroblast preparations of passage 2 (*lanes 3–5*). Expression of the proline 4-hydroxylase gene (*P4HB*) gene (~57 kDa) was used as fibroblast-specific loading control.

expressed in the absence or presence of $Ca_V1.2$ in COS cells (two experiments), arguing against the longevity of a pool of $Ca_V\beta2$ proteins not affected by *cacnb2* gene excision.

Current understanding of $Ca_V\beta$ function draws almost exclusively from heterologous expression of recombinant subunits in model systems, which may differ from cardiomyocytes. Studies in cardiomyocytes, in most cases, made use of overexpressing the neuronal rat $Ca_V\beta2a$ variant (3, 17), which is characterized by its intrinsic palmitoylation, although it is very unlikely the main $Ca_V\beta$ subunit associated with native cardiac calcium channels (2, 18, 19). This neuronal rat $Ca_V\beta2a$ (20) corresponds to $Ca_V\beta2$-N3, according to the nomenclature for human (19), mouse (2), and canine $Ca_V\beta2$ subunits (19), whereas the $Ca_V\beta2$ variant predominantly expressed in mouse heart is $Ca_V\beta2$-N4 (2, 19), which corresponds to human $Ca_V\beta2$-N4 (19) or $Ca_V\beta2b$ (21) and rabbit $Ca_V\beta2a$ (22).

Other strategies pursued to knock down endogenous cardiac $Ca_V\beta$ proteins were difficult to control because appropriate antibodies were not available in that study (23). Our results now indicate that in the adult mouse heart, $Ca_V\beta2$ is the most abun-

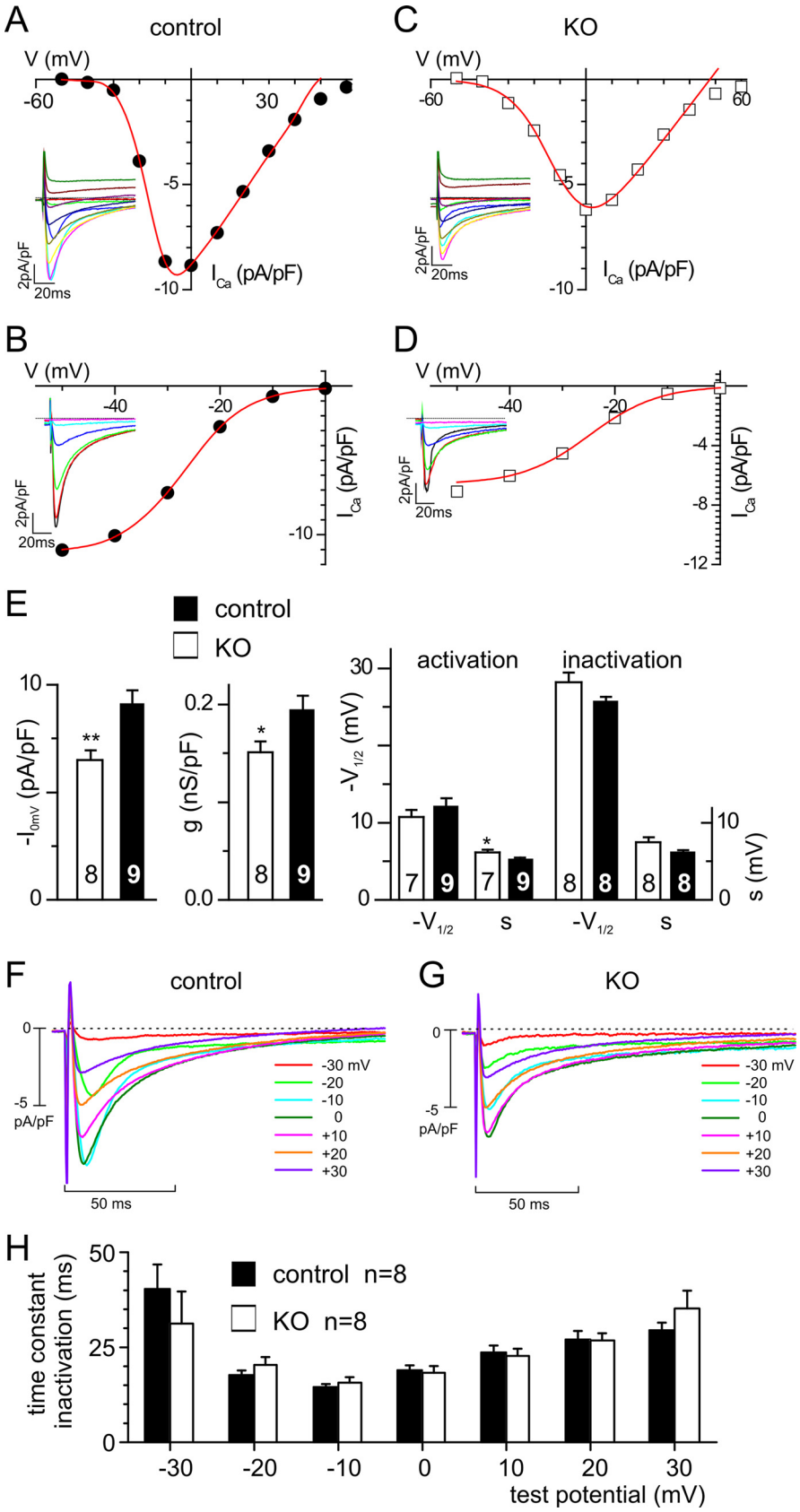

FIGURE 4. **Reduced I_{Ca} in adult cardiomyocytes from KO mice.** *A–G*, representative I_{Ca} and IV relations (*A* and *C*) and inactivation (*B* and *D*) in a control (*A* and *B*) and KO cardiomyocyte (*C* and *D*). *E*, summary. *, $p < 0.05$; **, $p < 0.005$. V indicates test potential (in *A* and *C*) and prepotential (in *B* and *D*), respectively. *F* and *G*, current families (*F*, controls; *G*, KO). Holding potential was −100 mV followed by a prestep of 100 ms to −40 mV and the test potentials after the prestep to the indicated voltages. Note that that the first part of all traces is the current at the −40 mV prepotential. *H*, summary of time constants of inactivation at the indicated potentials obtained from mono-exponential fits from *F* and *G*. No significant differences were measured between control and KO mice for all potentials ($p > 0.05$).

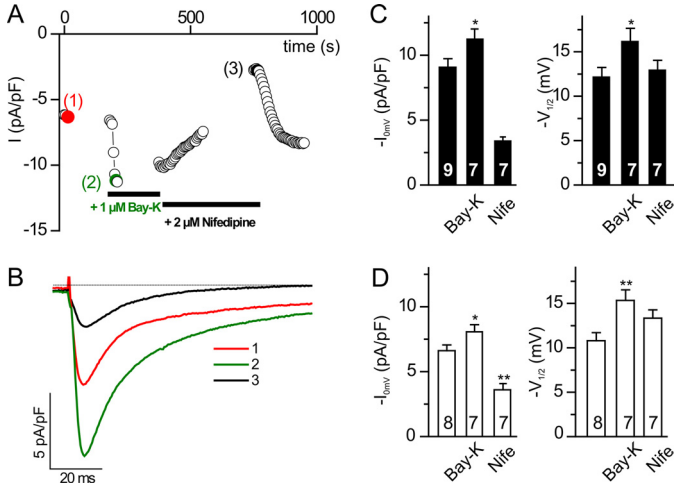

FIGURE 5. **Dihydropyridine sensitivity of I_{Ca} in cardiomyocytes.** *A* and *B*, representative I_{Ca} in the absence (**1**) and presence of Bay-K8644 (**2**) or nifedipine (**3**). *C* and *D*, current density and $V_{1/2}$act (mV) in the absence and presence of Bay-K8644 (*Bay-K*) or nifedipine (*Nife*) in control cells (*C*) and KO cells (*D*). *, $p < 0.05$.

dant $Ca_V\beta$, that $Ca_V\beta2$ is also expressed in cardiac fibroblasts, and that $Ca_V\beta2$ has an effect on calcium channel density similar to its effect on cardiomyocytes of mouse embryos. However, although it is essential for embryo survival, adult mice tolerate quite well the decrease of $Ca_V\beta2$.

Acknowledgments—We thank Christine Wesely, Stefanie Buchholz, Kerstin Fischer, and Christin Matka for expert technical assistance and Sabine Pelvay, Elisabeth Ludes, and Martin Jung for immunizing and bleeding rabbits.

REFERENCES

1. Dolphin, A. C. (2009) *Curr. Opin. Neurobiol.* **19,** 237–244
2. Link, S., Meissner, M., Held, B., Beck, A., Weissgerber, P., Freichel, M., and Flockerzi, V. (2009) *J. Biol. Chem.* **284,** 30129–30137
3. Nakayama, H., Chen, X., Baines, C. P., Klevitsky, R., Zhang, X., Zhang, H., Jaleel, N., Chua, B. H., Hewett, T. E., Robbins, J., Houser, S. R., and Molkentin, J. D. (2007) *J. Clin. Invest.* **117,** 2431–2444
4. Weissgerber, P., Held, B., Bloch, W., Kaestner, L., Chien, K. R., Fleischmann, B. K., Lipp, P., Flockerzi, V., and Freichel, M. (2006) *Circ. Res.* **99,** 749–757
5. Striessnig, J., and Koschak, A. (2008) *Channels* **2,** 233–251
6. Sohal, D. S., Nghiem, M., Crackower, M. A., Witt, S. A., Kimball, T. R., Tymitz, K. M., Penninger, J. M., and Molkentin, J. D. (2001) *Circ. Res.* **89,** 20–25
7. Murakami, M., Fleischmann, B., De Felipe, C., Freichel, M., Trost, C., Ludwig, A., Wissenbach, U., Schwegler, H., Hofmann, F., Hescheler, J., Flockerzi, V., and Cavalié, A. (2002) *J. Biol. Chem.* **277,** 40342–40351
8. Berggren, P. O., Yang, S. N., Murakami, M., Efanov, A. M., Uhles, S., Köhler, M., Moede, T., Fernström, A., Appelskog, I. B., Aspinwall, C. A., Zaitsev, S. V., Larsson, O., de Vargas, L. M., Fecher-Trost, C., Weissgerber, P., Ludwig, A., Leibiger, B., Juntti-Berggren, L., Barker, C. J., Gromada, J., Freichel, M., Leibiger, I. B., and Flockerzi, V. (2004) *Cell* **119,** 273–284
9. Badou, A., Jha, M. K., Matza, D., Mehal, W. Z., Freichel, M., Flockerzi, V., and Flavell, R. A. (2006) *Proc. Natl. Acad. Sci. U.S.A.* **103,** 15529–15534
10. Droogmans, G., and Nilius, B. (1989) *J. Physiol.* **419,** 627–650
11. Verrou, C., Zhang, Y., Zürn, C., Schamel, W. W., and Reth, M. (1999) *Biol. Chem.* **380,** 1435–1438
12. Obermair, G. J., Tuluc, P., and Flucher, B. E. (2008) *Curr. Opin. Pharmacol.* **8,** 311–318
13. Cantí, C., Davies, A., Berrow, N. S., Butcher, A. J., Page, K. M., and Dolphin, A. C. (2001) *Biophys. J.* **81,** 1439–1451
14. Berrow, N. S., Campbell, V., Fitzgerald, E. M., Brickley, K., and Dolphin, A. C. (1995) *J. Physiol.* **482,** 481–491
15. Catalucci, D., Zhang, D. H., DeSantiago, J., Aimond, F., Barbara, G., Chemin, J., Bonci, D., Picht, E., Rusconi, F., Dalton, N. D., Peterson, K. L., Richard, S., Bers, D. M., Brown, J. H., and Condorelli, G. (2009) *J. Cell Biol.* **184,** 923–933
16. Banerjee, I., Fuseler, J. W., Price, R. L., Borg, T. K., and Baudino, T. A. (2007) *Am. J. Physiol. Heart Circ. Physiol.* **293,** H1883–H1891
17. Jaleel, N., Nakayama, H., Chen, X., Kubo, H., MacDonnell, S., Zhang, H., Berretta, R., Robbins, J., Cribbs, L., Molkentin, J. D., and Houser, S. R. (2008) *Circ. Res.* **103,** 1109–1119
18. Wei, S. K., Colecraft, H. M., DeMaria, C. D., Peterson, B. Z., Zhang, R., Kohout, T. A., Rogers, T. B., and Yue, D. T. (2000) *Circ. Res.* **86,** 175–184
19. Foell, J. D., Balijepalli, R. C., Delisle, B. P., Yunker, A. M., Robia, S. L., Walker, J. W., McEnery, M. W., January, C. T., and Kamp, T. J. (2004) *Physiol. Genomics* **17,** 183–200
20. Perez-Reyes, E., Castellano, A., Kim, H. S., Bertrand, P., Baggstrom, E., Lacerda, A. E., Wei, X. Y., and Birnbaumer, L. (1992) *J. Biol. Chem.* **267,** 1792–1797
21. Takahashi, S. X., Mittman, S., and Colecraft, H. M. (2003) *Biophys. J.* **84,** 3007–3021
22. Hullin, R., Singer-Lahat, D., Freichel, M., Biel, M., Dascal, N., Hofmann, F., and Flockerzi, V. (1992) *EMBO J.* **11,** 885–890
23. Cingolani, E., Ramirez Correa, G. A., Kizana, E., Murata, M., Cho, H. C., and Marbán, E. (2007) *Circ. Res.* **101,** 166–175
24. Droogmans, G. (1997) *WinASCD*, Katholieke Universiteit Leuven, The Netherlands